https://doi.org/10.31891/2307-5732-2026-367-33
УДК 620.1:678.7

**VYTVYTSKYI VIKTOR**
National Technical University of Ukraine "Igor Sikorsky Kyiv Polytechnic Institute"
https://orcid.org/0000-0003-0184-3838
e-mail: vytvytskyi.v@gmail.com
**MIKULIONOK IHOR**
National Technical University of Ukraine "Igor Sikorsky Kyiv Polytechnic Institute"
https://orcid.org/0000-0001-8268-7229
e-mail: i.mikulionok@kpi.ua
**SOKOLSKYI OLEKSANDR**
National Technical University of Ukraine "Igor Sikorsky Kyiv Polytechnic Institute"
https://orcid.org/0000-0002-7929-3576
e-mail: sokolkiev@ukr.net
**SHVETS DANIIL**
National Technical University of Ukraine "Igor Sikorsky Kyiv Polytechnic Institute"
https://orcid.org/0009-0007-6758-883X
e-mail: schvezdania@gmail.com

# EFFECT OF REINFORCEMENT PARAMETERS ON THE STRESS–STRAIN STATE OF POLYMER COMPOSITE MASTS

*The aim of the study is to optimize the structure of a polymer composite with continuous longitudinal reinforcement for lighting masts by numerically simulating their stress–strain state under extreme wind loads.*

*A three-layer composite mast (epoxy matrix reinforced with fiberglass or carbon fiber) with an outer diameter of 90 mm, a wall thickness of 5 mm, and a height of 4 m was investigated. A comparison with the base aluminum structure (6060-T6 alloy) was performed using finite element analysis (FEA) in the Ansys software suite. The combined effect of storm wind (25 m/s), lighting device mass (5 kg), and aerodynamic pressure was taken into account. The volume fraction of fibers (40, 60, 80%) and the spatial location of the reinforced layer (inner, central, outer) in the cross-section were varied.*

*The use of polymer composites reduces the mast mass by 50–52% compared to the aluminum analogue (14.42 kg). Replacing fiberglass with carbon fiber additionally reduces the mass by ~10%. Increasing the fiberglass volume fraction from 40 to 80% increases the mass from 6.70 to 7.86 kg, reducing the maximum displacements of the mast top from 4.04 to 3.51 mm. The configuration with a reinforced inner layer provides the highest stiffness: deflections are 2.02–2.04 mm, equivalent stresses are 1.11–3.42 MPa, and the factor of safety reaches a maximum of 704–824. Reinforcing the outer layer increases equivalent stresses up to 5.22 MPa and reduces the factor of safety to ~260. Carbon fibers generate higher stresses (up to 5.22 MPa versus 3.03 MPa for fiberglass) due to a higher modulus of elasticity and local load concentration. Their higher strength limits (up to 2407 MPa) provide an average factor of safety (~575) close to that of fiberglass. The base aluminum mast has the smallest deflections (0.07 mm) but a significantly lower factor of safety (214). A structure with fiberglass in the inner layer at a volume fraction of 60–80% was determined to be rational for street lighting.*

*The patterns of local stiffness redistribution in tubular composite elements depending on the configuration of longitudinal continuous fibers were established. The possibility of targeted control of the mast strength without changing its geometry was proven, which is implemented in serial production using the developed direct extrusion technology.*

***Keywords:*** *mast, polymer composites, reinforcement, stress–strain state, numerical simulation, finite element analysis.*

**ВИТВИЦЬКИЙ ВІКТОР, МІКУЛЬОНОК ІГОР, СОКОЛЬСЬКИЙ ОЛЕКСАНДР, ШВЕЦЬ ДАНІІЛ**
Національний технічний університет України «Київський політехнічний інститут імені Ігоря Сікорського»

# ВПЛИВ ПАРАМЕТРІВ АРМУВАННЯ НА НАПРУЖЕНО-ДЕФОРМОВАНИЙ СТАН ПОЛІМЕРНО-КОМПОЗИТНИХ ЩОГЛ

*Метою дослідження є оптимізація структури полімерного композиту з неперервним поздовжнім армуванням для освітлювальних щогл шляхом числового моделювання їхнього напружено-деформованого стану за дії екстремальних вітрових навантажень.*

*Досліджено тришарову композитну щоглу (епоксидна матриця, армована скловолокном або вуглецевим волокном) із зовнішнім діаметром 90 мм, товщиною стінки 5 мм та висотою 4 м. Порівняння з базовою алюмінієвою конструкцією (сплав 6060-Т6) виконано методом скінченно-елементного аналізу (FEA) у комплексі Ansys. Враховано комбіновану дію штормового вітру (25 м/с), маси світильників (5 кг) та аеродинамічного тиску. Варіювали об'ємну частку волокон (40, 60, 80%) і просторове розташування армованого шару (внутрішній, середній, зовнішній) у поперечному перерізі.*

*Використання полімерних композитів знижує масу щогли на 50–52% порівняно з алюмінієвим аналогом (14,42 кг). Заміна скловолокна на вуглецеве додатково зменшує масу на ~10%. Збільшення об'ємної частки скловолокна з 40 до 80% збільшує масу з 6,70 до 7,86 кг, знижуючи максимальні переміщення вершини щогли з 4,04 до 3,51 мм. Конфігурація з армованим внутрішнім шаром забезпечує найвищу жорсткість: прогини становлять 2,02–2,04 мм, еквівалентні напруження – 1,11–3,42 МПа, а коефіцієнт запасу міцності досягає максимуму 704–824. Армування зовнішнього шару підвищує еквівалентні напруження до 5,22 МПа та знижує запас міцності до ~260. Вуглецеві волокна генерують вищі напруження (до 5,22 МПа проти 3,03 МПа для скловолокна) через вищий модуль пружності та локальну концентрацію навантажень. Їхні вищі ліміти міцності (до 2407 МПа) забезпечують близький до скловолокна середній запас міцності (~575). Базова алюмінієва щогла має найменші прогини (0,07 мм), але суттєво нижчий коефіцієнт запасу міцності (214). Раціональною для вуличного освітлення визначено структуру зі скловолокном у внутрішньому шарі при об'ємній частці 60–80%.*

*Встановлено закономірності перерозподілу локальної жорсткості трубчастих композитних елементів залежно від конфігурації поздовжніх неперервних волокон. Доведено можливість цілеспрямованого керування міцністю опор без зміни їхньої геометрії, що реалізується у серійному виробництві за допомогою розробленої технології прямотечійної екструзії.*

***Ключові слова:*** *щогла, полімерні композити, армування, напружено-деформований стан, числове моделювання, метод скінченних елементів.*

Стаття надійшла до редакції / Received 12.06.2026
Прийнята до друку / Accepted 17.07.2026
Опубліковано / Published 31.07.2026



## Introduction

For the lighting of various infrastructure, engineering structures such as lighting masts are widely used. Traditionally, lighting masts are manufactured from aluminum alloys or steel. This provides the necessary load-bearing capacity, but leads to a significant mass of the structure, high loads on the foundation, difficulties during transportation and installation, as well as vulnerability to corrosion. An alternative is polymer composites, which reduce the mass of load-bearing elements while maintaining stiffness, corrosion resistance, and durability [1, 2].

The application of finite element analysis (FEA) allows predicting the stress-strain state of composite structures, taking into account the volume fraction, spatial distribution of reinforcing fibers, cross-sectional geometry, and combined loads [3, 4]. For medium-height lighting masts, this approach enables the optimization of the polymer composite structure (fiber type, volume fraction, layer location). The main objective of such optimization is to minimize the mass of the structure while maintaining allowable deflections and the necessary factor of safety under storm winds.

## Literature Review

Replacing metal (steel and aluminum) poles with polymer composites significantly reduces the structural mass without losing load-bearing capacity and wind resistance [5, 6]. This is confirmed by the results of numerical strength evaluations of profiles, demonstrating the higher specific stiffness of composites compared to metals [6].

The effect of fiber volume fraction on the deformability and strength of composite elements has been investigated in [7–9]. An increase in the volume fraction improves the moduli of elasticity, strength, and fracture energy [9]. For vertical masts, optimizing the fiber fraction allows for minimizing bending deflections from wind with an insignificant increase in structural mass.

The spatial distribution of reinforcement is a critical strength factor. The local concentration of fibers redistributes stiffness, alters stress fields, and affects the ultimate load [10, 11]. Studies of the load-bearing capacity of polymer pipes with continuous longitudinal reinforcement confirm the determining influence of the fiber layers' location on the failure mode of the product [12, 13].

Carbon fibers outperform fiberglass in strength and stiffness at a lower density, but their cost is significantly higher [14, 15]. Carbon-epoxy composites exceed fiberglass systems in strength and modulus of elasticity by 20–70%, additionally providing a mass reduction of 10–20% [15].

The experience of applying composite masts in marine and tactical areas proves their operational advantages over metal ones: lower mass, corrosion resistance, and higher fatigue life [16, 17]. For onshore poles, the absence of corrosion additionally reduces maintenance costs, while the lower mass proportionally decreases the foundation load.

The fundamental aspects of the formation of the polymer matrix and reinforcing fibers, as well as the rheological behavior of melts, are based on the principles of polymer processing theory [18]. Based on these, for the practical implementation of composite masts, we have developed a direct extrusion die (Pat. UA153031U). Its design allows for introducing longitudinal fibers into the channel, varying their volume fraction and spatial location.

The operational reliability of extrusion equipment with similar design improvements, in particular, the strength of extrusion dies under melt pressure, has been confirmed by previous numerical studies [19], which guarantees the stability of the composite forming process.

The available literature confirms the feasibility of replacing metal load-bearing structures with polymer composites. However, the quantitative impact of structuring parameters (the interrelation of the location and volume fraction of longitudinal continuous fibers) on the stress-strain state of lighting masts remains insufficiently studied and requires further research.

## Goals of the Study

The aim of the study is a numerical evaluation of the stress-strain state of a polymer composite lighting mast (with continuous longitudinal reinforcement) and the comparison of its mass, stiffness, and factor of safety with a base aluminum structure.

To achieve this aim, the following tasks were set:

– to perform a finite element analysis of the composite mast's stress-strain state under storm wind conditions, taking into account the mass and area of lighting devices;

– to determine the effect of the reinforcing material type, fiber volume fraction, and location of the reinforced layer on the mast's mass, its maximum displacements, and the factor of safety;

– to justify rational reinforcement schemes based on the "mass/stiffness/factor of safety" criteria and to determine the areas of their practical application compared to existing aluminum and steel structures.

## Materials and Methods

### *Research Methodology*

A numerical simulation of the lighting mast's stress-strain state under storm wind was carried out in the Ansys software suite using finite element analysis (FEA). The adequacy of the selected approaches to numerical modeling, in particular the configuration of mesh domains and boundary conditions, is based on verified methodologies from previous works by the authors [20, 21].

A comparison of the calculation results was performed for the base mast made of an aluminum alloy and the improved mast made of a polymer composite reinforced with continuous longitudinal fibers. Additionally, the effect of the volume concentration and fiber layer structure in the cross-section on the stress-strain state of the mast was investigated.

Examples of typical lighting mast structures are shown in Figure 1.


**Fig.1. Typical lighting masts**

***Geometry and Materials***

The mast body was modeled as a thin-walled cylindrical shell with an outer diameter $D$ = 90 mm (0.09 m), a wall thickness $t$ = 5 mm (0.005 m), and a height $H$ = 4 m.

The finite element mesh of the modeled lighting mast was specified with a finite element size of 20 mm along the structure's height and 1 mm in thickness. The selection of the mesh domain parameters was justified by comparing modeling results with different element sizes until an acceptable convergence of up to 5% was achieved.

The base mast material is the 6060-T6 aluminum alloy with mechanical properties typical of 6060/6063-T5/T6 alloys (Table 1) [22], which is widely used in lighting masts due to its high specific strength and corrosion resistance [1].

Table 1

**Material properties**

| Material | Axis | $E$, MPa | ν | $G$, MPa | ρ, kg/m³ | $\sigma_{\text{т}}$, MPa | $\sigma_{\text{в}}$, MPa |
|---|---|---|---|---|---|---|---|
| Aluminum 6060-T6 | *x,y,z* | 70 000 | 0.33 | 26 300 | 2700 | 210 | 240 |
| Epoxy resin | *x,y,z* | 2500 | 0.33 | 940 | 1100 | 40 | 70 |
| Fiberglass | *x* | 20 000 | $\nu_{xy}$ = 0.25 | $G_{xy}$ = 0.25 | 2540 | – | – |
| | *y* | 20 000 | $\nu_{xz}$ = 0.22 | $G_{xz}$ = 0.22 | | – | – |
| | *z* | 72 000 | $\nu_{yz}$ = 0.22 | $G_{yz}$ = 0.22 | | 2000 | 2000 |
| Carbon fiber (high-strength) | *x* | 15 000 | $\nu_{xy}$ = 0.40 | $G_{xy}$ = 0.40 | 1900 | – | – |
| | *y* | 15 000 | $\nu_{xz}$ = 0.27 | $G_{xz}$ = 0.27 | | – | – |
| | *z* | 240 000 | $\nu_{yz}$ = 0.27 | $G_{yz}$ = 0.27 | | 3000 | 3000 |

In table 1: $E$ – tensile modulus of elasticity, MPa; ν – Poisson's ratio; $G$ – shear modulus, MPa; ρ – density, kg/m³; $\sigma_{\text{т}}$ – tensile yield strength, MPa; $\sigma_{\text{в}}$ – ultimate tensile strength, MPa.

An epoxy resin with typical properties was used as the matrix polymer for manufacturing the polymer composite mast (Table 1) [23]. Carbon fiber and fiberglass were used for reinforcement. The physical and mechanical properties of the reinforcing fibers as an independent element (without matrix) were set using average standard values (Table 1) based on experimental studies [24, 25].

The polymer composite mast was modeled as a three-layer structure (inner, central, and outer layers). The volume content of continuous longitudinal fibers was set at 40, 60, and 80% for one of the layers in turn. This allowed investigating the effect of the reinforcement structure on the stress-strain state of the structure.

The main characteristics of the composite layer were determined according to the author's methodology [12]. When setting the orthotropic properties of the fibers, the direction of the mast axis along the global z-axis was taken into account.

***Loads and Boundary Conditions***

In the finite element model (FEA), the following forces were taken into account to investigate the mast under combined loading (Figure 2):

– load from lighting devices on the mast (B);
– wind load on the mast (C);
– wind load on the lighting devices (E);
– standard Earth gravity (D).

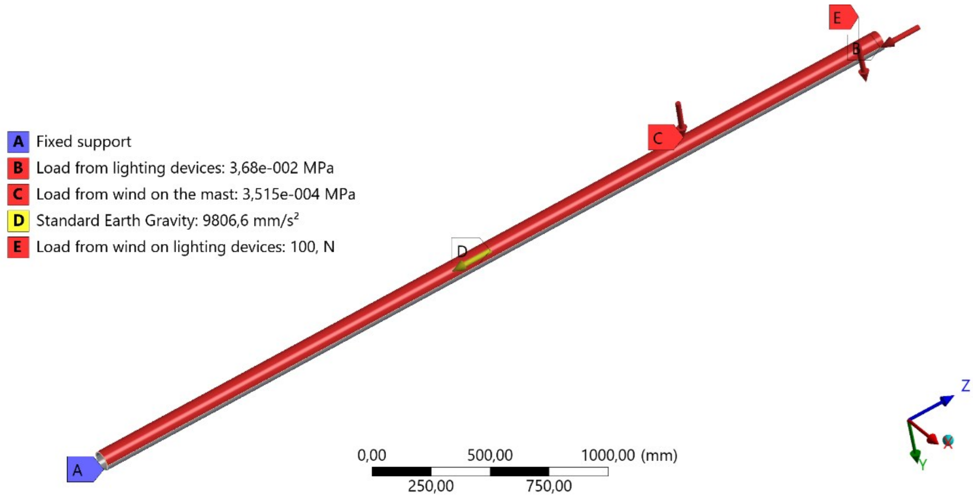


**Fig.2. Simulation model with loads and boundary conditions**

Boundary conditions: the lower end of the mast was rigidly fixed using a cantilever scheme (Figure 2, A), which simulates the actual mounting in the foundation.

***Load from lighting devices***

The installation of LED street luminaires with a mass of 1–2.5 kg (power of 50–150 W) was modeled [26, 27]. The luminaires were not modeled geometrically: their weight was replaced by an equivalent pressure applied to the upper end of the mast along the vertical z-axis, directed downwards along the mast axis.

For the calculation, the total mass of the lighting devices $m_{\text{lamps}}$ = 5 kg was assumed. The corresponding vertical force

$$F_{\text{lamps}} = m_{\text{lamps}} g = 5 \cdot 9.81 \approx 49.05 \text{ H}. \tag{1}$$

Cross-sectional area of the wall

$$S_{\text{cyl}} = \frac{\pi}{4}\left(D^2 - (D-2t)^2\right) = \frac{\pi}{4}\left(0.09^2 - 0.08^2\right) \approx 1.335 \cdot 10^{-3} \text{ м}^2. \tag{2}$$

Equivalent pressure from the luminaires' weight

$$p_{\text{lamps}} = \frac{F_{\text{lamps}}}{S_{\text{cyl}}} \approx \frac{49.05}{1.335 \cdot 10^{-3}} \approx 36800 \text{ Па}. \tag{3}$$

***Load from wind on the mast***

Storm conditions with a wind speed $V$ = 25 m/s, which corresponds to a severe storm on the Beaufort scale (10 points), were modeled [28]. The range of 24.5…28.4 m/s is representative for calculating extreme wind loads on high-rise structures [29].

The dynamic wind pressure on the mast shaft was determined by the formula [30]

$$q_{\text{w}} = 0.5\rho_{\text{w}} V^2 = 0.5 \cdot 1.25 \cdot 25^2 = 390.6 \text{ Па}, \tag{4}$$

where $\rho_{\text{w}}$ = 1.25 kg/m$^3$ is the air density.

For a cylindrical mast with an aerodynamic coefficient $C_{\text{cyl}}$ = 0.9 [31], the equivalent pressure was applied to the windward half of the mast's lateral surface according to the methodology [32, 33], which approximately replicates the effect of wind from one side. The wind pressure on the mast was calculated as follows

$$p_{\text{w}} = C_{\text{cyl}} q_{\text{w}} = 0.9 \cdot 390.6 \approx 351.5 \text{ Па}. \tag{5}$$

***Load from wind on lighting devices***

To account for the wind load on the lighting devices, the frontal contour of the luminaires was approximated by rectangles of 0.5×0.2 m (projected area $S_{\text{lamp}} \approx$ 0.10 m²) [23, 34]. Taking into account the aerodynamic drag coefficient for a flat body $C_{\text{corps}} \approx$ 1.2 [31], the equivalent pressure on the luminaire is

$$p_{\text{corps}} = C_{\text{corps}} q_{\text{w}} \approx 1.2 \cdot 390.6 \approx 468.7 \text{ Па}. \tag{6}$$

The total load from two luminaires

$$F_{\text{total}} = 2 p_{\text{corps}} S_{\text{lamp}} \approx 2 \cdot 468.7 \cdot 0.10 \approx 100 \text{ H}. \tag{7}$$

In the calculation model, this force was applied at the mounting point of the luminaires ($h$ = 3.9 m) along the normal to the lateral wall of the mast in the direction of the wind (y-axis)

**Results and Discussion**

The numerical simulation of the lighting mast's stress-strain state provided the following results (table 2)

Table 2

**Numerical simulation results**

| Material type | Content, % | Layer | *m*, kg | $\sigma_{eq}$, MPa | ε, mm/mm | $\delta_{tot}$, mm | $\sigma_{lim}$, MPa | FoS |
|---|---|---|---|---|---|---|---|---|
| Fiberglass + Epoxy resin | 40 | Central | 6.62 | 2.44 | 0.1909 | 5.07 | 821 | 336 |
| | | Inner | 6.83 | 1.11 | 0.0596 | 2.04 | 821 | 737 |

| | | | | | | | | |
|---|---|---|---|---|---|---|---|---|
| | | Outer | 6.65 | 2.24 | 0.1937 | 5.02 | 821 | 366 |
| Carbon fibre + Epoxy resin | 40 | Central | 6.21 | 2.44 | 0.2032 | 5.04 | 1221 | 500 |
| | | Inner | 6.30 | 1.60 | 0.0629 | 2.04 | 1221 | 763 |
| | | Outer | 6.22 | 4.68 | 0.2046 | 4.99 | 1221 | 260 |
| Fiberglass + Epoxy resin | 60 | Central | 7.14 | 2.31 | 0.1677 | 4.62 | 1214 | 525 |
| | | Inner | 7.50 | 1.47 | 0.0571 | 2.04 | 1214 | 824 |
| | | Outer | 7.19 | 2.10 | 0.1293 | 3.97 | 1214 | 578 |
| Carbon fibre + Epoxy resin | 60 | Central | 6.53 | 2.79 | 0.1748 | 4.58 | 1814 | 649 |
| | | Inner | 6.71 | 2.24 | 0.0588 | 2.03 | 1814 | 810 |
| | | Outer | 6.55 | 3.59 | 0.1383 | 3.94 | 1814 | 504 |
| Fiberglass + Epoxy resin | 80 | Central | 7.67 | 3.01 | 0.1482 | 4.56 | 1607 | 533 |
| | | Inner | 8.17 | 2.18 | 0.0516 | 2.03 | 1607 | 738 |
| | | Outer | 7.73 | 3.03 | 0.1149 | 3.93 | 1607 | 530 |
| Carbon fibre + Epoxy resin | 80 | Central | 6.85 | 4.59 | 0.1544 | 4.48 | 2407 | 524 |
| | | Inner | 7.12 | 3.42 | 0.0530 | 2.02 | 2407 | 704 |
| | | Outer | 6.88 | 5.22 | 0.1217 | 3.87 | 2407 | 461 |
| Base Aluminum | - | - | 14.42 | 1.12 | $2.15 \cdot 10^{-5}$ | 0.07 | 240 | 214 |

In table 2: *m* – mast mass, kg; $\sigma_{eq}$ – equivalent (von Mises) stress, MPa; ε – equivalent strain, mm/mm; $\delta_{tot}$ – total displacement, mm; $\sigma_{lim}$ – calculated strength limit, MPa; FoS – factor of safety.

Based on the numerical simulation results, the use of polymer composites reduces the mast mass by 50–52% compared to the base aluminum structure (14.42 kg). The mass of the composite masts ranges from 6.21 to 8.17 kg. Replacing fiberglass with carbon fiber additionally reduces the mass by ~10% (from 7.28 kg to 6.60 kg on average). This confirms the higher "stiffness-to-mass" ratio for carbon polymer composites, which is characteristic of such structural elements [8].

The volume fraction of reinforcement directly affects the mass and deformability of the structure. With an increase in the fiberglass fraction from 40% to 80%, the mass increases from 6.70 kg to 7.86 kg, and for carbon fiber – from 6.24 kg to 6.95 kg. At the same time, the maximum displacements of the mast top decrease: from 4.04 mm to 3.51 mm for fiberglass and from 4.02 mm to 3.46 mm for carbon fiber. Thus, an increase in the fiber fraction predictably improves the mast's stiffness due to a moderate mass increase, which is consistent with the data [7, 34].

The location of the reinforced layer determines the stress-strain state of the structure. The smallest displacements (2.02–2.04 mm) and equivalent stresses (1.11–3.42 MPa) were obtained for configurations with a reinforced inner layer (FoS = 704–824). Reinforcing the outer layer leads to an increase in stresses (up to 5.22 MPa) and deflections (up to 5.02 mm), reducing the FoS to ~260. Configurations with a central layer demonstrate intermediate values. This sensitivity to position change confirms the influence of the spatial distribution of reinforcement on the local stiffness of the cross-section [11, 12].

At the same fiber volume fraction, the materials demonstrate different stress values. For fiberglass, the equivalent stresses do not exceed 3.03 MPa. For carbon fiber, they reach 5.22 MPa due to a higher modulus of elasticity and the corresponding load concentration in the composite. However, the strength limits of carbon fiber are significantly higher (up to 2407 MPa versus 1607 MPa for fiberglass). This provides close average FoS values (~575) for both options. The transition to carbon fiber further reduces mass but requires consideration of higher local stresses when evaluating failure mechanisms [14, 35].

The base aluminum mast has the smallest deformations (0.07 mm), but its factor of safety is 214, which is lower than the values for composite configurations. The deformations of composite masts are higher (2.02–5.07 mm), but they remain within operational tolerances. Poles reinforced with composite fibers provide a higher factor of safety with a significant mass reduction, which is consistent with the results of numerical and experimental studies of similar structures [5, 36].

## Conclusions and Future Work

Replacing aluminum alloy with polymer composites in lighting mast structures ensures a 50–52% reduction in mass and an increase in the factor of safety. Such a weight reduction decreases the load on the foundation and fasteners, simplifies transportation, allows installation without heavy lifting equipment, and reduces construction and installation costs.

The use of carbon fiber is justified for structures with strict requirements for mass and dynamic stability (storm winds, vibrations), despite the higher material cost. For mass street lighting, fiberglass reinforcement (fiber volume fraction of 60–80%, reinforced inner layer) can be optimal in terms of the "strength/cost" ratio. This configuration provides a high FoS, operational stiffness, and minimizes maintenance costs due to corrosion resistance and the lack of a need for regular painting.

Future research will focus on scaling the obtained results for high-rise masts (telecommunication, navigation, power transmission, and marine poles). For such structures, reducing the mass of the upper part without loss of strength is critical for ensuring stability, which is fully consistent with the trends in using polymer composites in marine and military applications [17]. The next stages of work will include optimizing reinforcement schemes for different heights, studying fatigue and corrosion durability in actual climatic conditions, and evaluating the life cycle cost of composite poles compared to metal ones.

**References**


1. Unicomposite. (2025). *The advantages of FRP lighting pole*. Retrieved from https://www.unicomposite.com/the-advantages-of-frp-lighting-pole

2. Love, L., Post, B., Tekinalp, H., Wang, P., Atkins, C., Roschli, A., Zhao, X., & Rencheck, M. (2021). *Assessment of commercial composite power pole performance* (Report No. ORNL/TM-2021/2068). Oak Ridge National Laboratory. Retrieved from https://info.ornl.gov/sites/publications/Files/Pub160200.pdf

3. Guo, Q., Yao, W., Li, W., & Gupta, N. (2021). Constitutive models for the structural analysis of composite materials for the finite element analysis: A review of recent practices. *Composite Structures*, *256*, 113267. doi:10.1016/j.compstruct.2020.113267

4. Müzel, S. D., Bonhin, E. P., Guimarães, N. M., & Guidi, E. S. (2020). Application of the finite element method in the analysis of composite materials: A review. *Polymers*, *12*(4), 818. doi:10.3390/polym12040818

5. Lonare, A. U., Banpurkar, R., & Gautam, R. (2020). Design & failure analysis of solar street light pole under wind load effect. *International Research Journal of Engineering and Technology (IRJET)*, *7*(4), 2724.

6. Abdulqadir, S. F., Alaseel, B. H., & Sameer, J. O. (2024). Comparison of the mechanical properties and approach to numerical modeling of fiber-reinforced composite, high-strength steel and aluminum. *Journal of Engineering and Technological Sciences*, *56*(1). doi:10.5614/j.eng.technol.sci.2023.56.1.9

7. Esnaola, A., Tena, I., Aurrekoetxea, J., Gallego, I., & Ulacia, I. (2016). Effect of fibre volume fraction on energy absorption capabilities of E-glass/polyester automotive crash structures. *Composites Part B: Engineering*, *85*, 1–7. doi:10.1016/j.compositesb.2015.09.007

8. Jacob, G. C., Starbuck, J. M., Fellers, J. F., & Simunovic, S. (2005). Effect of fiber volume fraction, fiber length and fiber tow size on the energy absorption of chopped carbon fiber–polymer composites. *Polymer Composites*, *26*, 293–305. doi:10.1002/pc.20100

9. Dinesha, V. C. (2019). Effect of fiber orientation and volume fraction on the impact resistance of bio-composites. *World Journal of Advanced Research and Reviews*, *2*(3), 067–075. doi:10.30574/wjarr.2019.2.3.0141

10. Liu, C., Li, H., Wang, M., Zou, H., Xu, X., & Xiong, L. (2025). Experimental and numerical simulation of the ultimate bearing capacity of steel pipe components reinforced with ribbed sleeves under axial and eccentric compression. *Engineering Failure Analysis*, 110134. doi:10.1016/j.engfailanal.2025.110134

11. Pyskunov, S., & Bakhtovarshoiev, T. (2025). Stress–strain state and elastic properties of composites with variable reinforcement structure. *Scientific Journal of the Ternopil National Technical University*, *119*(3), 127–133. doi:10.33108/visnyk_tntu2025.03.127

12. Vytvytskyi, V., Sokolskyi, O., & Mikulionok, I. (2026). Numerical analysis of the ultimate load-bearing capacity of polymer pipes reinforced with continuous longitudinal fibers. *Transactions of Kremenchuk Mykhailo Ostrohradskyi National University, 2*(1(156)), 83–90. doi:10.32782/1995-0519.2026.1.2.10

13. Karvatskii, A., Lazarev, T., Mikulionok, I., Vytvytskyi, V., & Solovei, V. (2021). Mathematical modeling of physical and mechanical properties of polymeric materials reinforced with carbon nanotubes. In V. Ivanov, I. Pavlenko, O. Liaposhchenko, J. Machado, & M. Edl (Eds.), *Advances in design, simulation and manufacturing IV: DSMIE 2021 (Lecture Notes in Mechanical Engineering)*. Springer. doi:10.1007/978-3-030-77823-1_4

14. Al-Qrimli, H. F., Mahdi, F. A., & Ismail, F. B. (2015). Carbon/epoxy woven composite experimental and numerical simulation to predict tensile performance. *Advances in Materials Science and Applications, 4*(2), 33–41. doi:10.5963/AMSA0402001

15. PartMFG. (2024, December 31). *Carbon fiber vs fiberglass – a comparative analysis*. Retrieved from https://www.partmfg.com/carbon-fiber-vs-fiberglass-a-comparative-analysis

16. Rustler Yachts. (n.d.). *How a carbon fibre mast benefits a cruising yacht*. Retrieved from https://www.rustleryachts.com/carbon-v-aluminium-masts

17. Mastsystem. (2024, September 2). *Composite mast vs. aluminum mast: Which mast system offers better performance for tactical applications?* Retrieved from https://www.mastsystem.com/news/composite-mast-vs-aluminum-mast

18. Mikulionok, I. O. (2025). Tekhnolohiia pereroblennia polimeriv [Polymer processing technology]. Igor Sikorsky Kyiv Polytechnic Institute. Retrieved from https://ela.kpi.ua/handle/123456789/74268

19. Vytvytskyi, V., Oleksyshen, V., & Shvets, D. (2026). Finite element strength analysis of an extruder die with design modifications [in Ukrainian]. *Bulletin of NTUU «Igor Sikorsky Kyiv Polytechnic Institute», Series «Chemical Engineering, Ecology and Resource Saving»*, (2), 38–44. doi:10.20535/2617-9741.2.2026.365626

20. Karvatskyi, A. Ya., Omelchuk, I. V., Mikulionok, I. O., & Vytvytskyi, V. M. (2020). Investigation of the physical properties of polymers by molecular dynamics and using LAMMPS (Review). *Bulletin of NTUU «Igor Sikorsky Kyiv Polytechnic Institute», Series «Chemical Engineering, Ecology and Resource Saving»*, (4), 17–28. doi:10.20535/2617-9741.4.2020.219780

21. Vytvytskyi, V., Vytvytskyi, Vl., Mikulionok, I., Sokolskyi, O., & Shylovych, T. (2023). Study of the modernized single-screw extruder body energy efficiency. *Bulletin of NTUU «Igor Sikorsky Kyiv Polytechnic Institute», Series «Chemical Engineering, Ecology and Resource Saving»*, (4), 9–17. doi:10.20535/2617-9741.4.2023.294323

22. Extrusion.com.ua. (n.d.). Selection of alloy for aluminum profile extrusion (alloy 6060/6063). Retrieved from https://extrusion.com.ua/uk/aluminium-alloy

23. Wan, X., Demir, B., An, M., Walsh, T. R., & Yang, N. (2021). Thermal conductivities and mechanical properties of epoxy resin as a function of the degree of cross-linking. *arXiv*. doi:10.48550/arXiv.2104.02430

24. Ilankeeran, P. K., Mohite, P. M., & Kamle, S. (2012). Axial tensile testing of single fibres. *MME – Modeling and Numerical Simulation of Material Science, 2*(4), 151–156. doi:10.4236/mme.2012.24020

25. Park, S. J., & Seo, M. K. (2011). Element and processing. In S. J. Park & M. K. Seo (Eds.), *Interface science and composites* (Interface Science and Technology, Vol. 18, pp. 431–499). Elsevier. doi:10.1016/B978-0-12-375049-5.00006-2

26. Ledster. (n.d.). *VS-STL-S-150W LED street luminaire*. Retrieved from https://ledster.com.ua/ulichnie_led_fonari/vs_stl_s_150w.html

27. Sunled. (n.d.). *Street LED luminaire 50 W SMD Econom*. Retrieved from https://sunled.ua/vulichne_osvitlennya/vulichnij-lihtar-50-vt-smd-ekonom-sll-50-cob-e-smd-ua

28. Atom. (2025, March 12). *What is the Beaufort scale and how is it used?* Retrieved from https://anclademia.com/en/blog/que-es-la-escala-beaufort-y-como-se-usa

29. Aestech. (2026, March 31). *Wind and construction: How to bring them together*. Retrieved from https://aestech.com/en/news/wind-and-construction-how-to-bring-them-together

30. Leappole. (2025, November 7). Light pole wind load and structural strength test. Retrieved from https://www.leappole.com/blog/light-pole-wind-load-and-structural-strength-test

31. Scribd. (n.d.). *Wind load calculations for light poles*. Retrieved from https://www.scribd.com/document/462704367/wind-load-calculation-9-mtr

32. Ministry of Construction of Ukraine. (2026). *DBN V.1.2-2:2006. Loads and actions. Design standards*. Retrieved from https://e-construction.gov.ua/laws_detail/3875993677809583397

33. Pichugin, S. F. (2023). *Method of limit states and calculation of building structures* [Textbook]. Retrieved from https://reposit.nupp.edu.ua/files/original/10/11200/75ce46af11326c56ef80c7b0f4b100a912f28494.pdf

34. Baskutis, S., Nariūnas, M., & Baskutienė, J. (2014). The fiber volume fraction influence on mechanical properties of multi-layered carbon tubes. *Mechanika, 20*(6), 543–549. doi:10.5755/j01.mech.20.6.8880

35. Lawrence, B. D., Coatney, M. D., Phillips, F., Henry, T. C., Nikishkov, Y., & Makeev, A. (2022). Evaluation of the mechanical properties and performance cost of additively manufactured continuous glass and carbon fiber composites. T*he International Journal of Advanced Manufacturing Technology, 120*, 1135–1147. doi:10.1007/s00170-022-08879-w

36. Broniewicz, M., Broniewicz, F., & Broniewicz, E. (2025). Experimental and numerical verification of the standard procedure for determining the load capacity of GFRP composite lighting columns. *Archives of Civil Engineering, LXXI*(1), 381–401. doi:10.24425/ace.2025.153340